Pergamon

www.elsevier.com/locate/neuroscience

PII: S0306-4522(00)00453-X

Neuroscience Vol. 102, No. 1, pp. 229–240, 2001

0306-4522/01 $20.00+0.00

CONTRIBUTION OF PRESYNAPTIC CALCIUM-ACTIVATED POTASSIUM CURRENTS TO TRANSMITTER RELEASE REGULATION IN CULTURED *XENOPUS* NERVE–MUSCLE SYNAPSES

J. M. PATTILLO,[a] B. YAZEJIAN,[b] D. A. DIGREGORIO,[b] J. L. VERGARA,[b] A. D. GRINNELL[b] and S. D. MERINEY[a]*

[a]Department of Neuroscience, University of Pittsburgh, Pittsburgh, PA 15260, USA

[b]Department of Physiology, Jerry Lewis Neuromuscular Research Center, University of California at Los Angeles, School of Medicine, Los Angeles, CA 90095, USA

Abstract—Using *Xenopus* nerve–muscle co-cultures, we have examined the contribution of calcium-activated potassium (K_{Ca}) channels to the regulation of transmitter release evoked by single action potentials. The presynaptic varicosities that form on muscle cells in these cultures were studied directly using patch-clamp recording techniques. In these developing synapses, blockade of K_{Ca} channels with iberiotoxin or charybdotoxin decreased transmitter release by an average of 35%. This effect would be expected to be caused by changes in the late phases of action potential repolarization. We hypothesize that these changes are due to a reduction in the driving force for calcium that is normally enhanced by the local hyperpolarization at the active zone caused by potassium current through the K_{Ca} channels that co-localize with calcium channels. In support of this hypothesis, we have shown that when action potential waveforms were used as voltage-clamp commands to elicit calcium current in varicosities, peak calcium current was reduced only when these waveforms were broadened beginning when action potential repolarization was 20% complete. In contrast to peak calcium current, total calcium influx was consistently increased following action potential broadening. A model, based on previously reported properties of ion channels, faithfully reproduced predicted effects on action potential repolarization and calcium currents.

From these data, we suggest that the large-conductance K_{Ca} channels expressed at presynaptic varicosities regulate transmitter release magnitude during single action potentials by altering the rate of action potential repolarization, and thus the magnitude of peak calcium current. © 2001 IBRO. Published by Elsevier Science Ltd. All rights reserved.

Key words: BK, action potential, iberiotoxin, charybdotoxin, neuromuscular.

Neurotransmitter release is critically dependent on the entry of calcium through voltage-dependent calcium channels localized to active zone regions of the nerve terminal.[5,27,34] The magnitude and time course of calcium entry during an action potential (AP) are very sensitive to the rate of repolarization.[3,50,64,67] In this context, the gating of potassium channels is important, since they shape the repolarization and afterhyperpolarization. Blockade of voltage-gated potassium channels has been shown to cause AP broadening, which increases calcium influx and enhances neurotransmitter release.[3,50,67] Large-conductance K_{Ca} (BK) channels are of particular interest, since they have been shown to be selectively expressed at nerve terminals[6,32,49,53,65] and are co-localized with calcium channels in the active zone.[47,49,68] Their open probability is increased upon binding calcium,[36] and in some preparations they can open during a single AP.[1,30,33,47,68] Since they can open during AP repolarization at synapses, BK channels are hypothesized to accelerate AP repolarization and terminate transmitter release. At mature frog neuromuscular synapses, for example, BK channel blockade increases transmitter release.[48] When examined at the soma, blockade of BK channels has been shown to broaden APs beginning at various times during the repolarization phase, and to decrease the size of the afterhyperpolarization.[14,45,51,52,55,59,70]

To study directly the role of BK channels in nerve terminals, it is desirable to have access to the presynaptic nerve terminal for electrophysiological recording. Several preparations have been developed that allow direct study of presynaptic ionic currents and transmitter release.[4,6,9–11,22,31,34,54,57,62] Recently, the presynaptic varicosities that form on muscle cells in co-cultures of *Xenopus laevis* spinal neurons and muscle have been used for the direct study of presynaptic ionic currents and transmitter release.[68] This *Xenopus* nerve–muscle co-culture preparation has previously been used to study presynaptic sodium,[29] calcium[26,38,68] and calcium-activated potassium currents, as well as calcium current coupling to transmitter release.[68,69] In this study, we test the hypothesis that synaptic BK channels play a role in

*Corresponding author. Tel.: +1-412-624-8283; fax: +1-412-624-9198.
E-mail address: meriney@bns.pitt.edu (S. D. Meriney).

Abbreviations: ACh, acetylcholine; AP, action potential; BK, large-conductance, calcium-activated potassium (channel); ChTX, charybdotoxin; 3,4-DAP, 3,4-diaminopyridine; EGTA, ethyleneglycol-bis(β-aminoethyl ether)-*N*,*N*,*N*′,*N*′-tetra-acetate; EPC, endplate current; HEPES, *N*-2-hydroxyethylpiperazine-*N*′-2-ethanesulfonic acid; IBTX, iberiotoxin; mEPC, miniature endplate current; NFR, normal frog Ringer.

regulating transmitter release at cultured *Xenopus* nerve–muscle synapses.

EXPERIMENTAL PROCEDURES

Xenopus *nerve–muscle cultures*

Fertilized eggs of *Xenopus laevis* were allowed to develop to stages 22–23[42] and cultures were made as described previously.[61,68] The cultures were maintained at room temperature in a defined medium containing either 40% Iscove's modified Dulbecco's medium or L-15 (Sigma, St Louis, MO), 50% normal frog Ringer (NFR) and 10% deionized H_2O, supplemented with insulin, sodium selenite, transferrin, penicillin–streptomycin and brain-derived neurotrophic factor (50 ng/ml; kindly provided by Regeneron, Tarrytown, NY, and Amgen, Thousand Oaks, CA). Recordings were made from neuritic presynaptic varicosities and postsynaptic myocytes in one- to two-day-old cultures. Before recording, the culture medium was replaced by the appropriate bath solution.

Endplate current recordings

For recording of endplate currents (EPCs) in myocytes, the traditional whole-cell patch-clamp technique was used. The internal whole-cell solution consisted of (in mM): 100 KCl, 20 HEPES, 11 EGTA, 1 $CaCl_2$, 1 $MgCl_2$ (pH 7.4). Occasionally, the intracellular sodium channel blocker QX-314[21] was added to the whole-cell solution at a final concentration of 5 mM. NFR (in mM: 116 NaCl, 3 KCl, 20 HEPES, 1.8 $CaCl_2$, 2 $MgCl_2$) was used as the control bath for recording of EPCs.

Transmitter release was evoked (at 0.066 Hz) by one of three methods of nerve stimulation: current injection during whole-cell patch-clamp recordings from the presynaptic varicosity or neuron somata, or extracellular stimulation of the presynaptic motoneuron somata. A polished pipette filled with bath solution was pushed against the soma cell membrane to stimulate the neuron extracellularly. A Grass stimulator (S-48) and stimulus isolation unit were used to deliver 0.5–1.5-μA pulses which were 0.01–0.1 ms in duration. The traditional whole-cell technique in fast current-clamp mode was used to stimulate the neuron soma (0.5–2 nA, 0.5 ms). The internal pipette solution for neurons consisted of (in mM): 110 KCl, 1 $MgCl_2$, 1 NaCl, 10 HEPES (pH 7.4). Mg-ATP (4 mM) and Na-GTP (0.3 mM) were added fresh daily. The perforated patch whole-cell technique in current-clamp mode was used to stimulate the presynaptic varicosity. The internal pipette solution for varicosities consisted of (in mM): 52 K_2SO_4, 38 KCl, 1 K-EGTA, 5 HEPES (pH 7.2), plus 400–600 μg/ml amphotericin-B.

Action potential recordings

APs were recorded from varicosities using the perforated patch technique in "fast" current-clamp mode[35] on an Axopatch 200A patch-clamp amplifier (Axon Instruments, Foster City, CA). APs were activated with current injection (at 0.2 Hz) directly into the varicosity (0.35–1.3 nA for 0.5 ms). The pipette solution consisted of (in mM): 60 K_2SO_4, 45 KCl, 8 $MgCl_2$, 10 HEPES (pH 7.4). Cultures were bathed in NFR before recording. The pipette tip was dipped in the above solution for 3–5 s and then back-filled with this solution plus 400 μg/ml amphotericin-B (Sigma, St Louis, MO).[46] Only varicosities that were clearly in contact with myocytes were selected for recording. Occasionally, α-bungarotoxin (5 μg/ml) was focally applied to prevent twitching of the postsynaptic myocyte. The resting potential of varicosities varied between −70 and −50 mV. A small amount of steady current (<100 pA) was sometimes injected to keep the resting potential near −60 mV.

Calcium current recordings

Recordings of calcium current in *Xenopus* neuron somata and varicosities were made using the amphotericin-B perforated patch-clamp technique, as described above. For recordings of calcium current from neuron somata, the perforated patch pipette solution consisted of (in mM): 68 $CsMeSO_4$, 50 CsCl, 8$MgCl_2$, 10 HEPES (pH 7.4), and the bath solution consisted of (in mM): 90 NaCl, 10 $CaCl_2$, 1 $MgCl_2$, 5 HEPES, 20 tetraethylammonium chloride, 5 3,4-diaminopyridine (3,4-DAP), 1 μM tetrodotoxin (pH 7.4). Step pulses to +20 mV from a holding potential of −80 mV were used to evoke calcium currents. For recordings of calcium current from varicosities, the perforated pipette solution consisted of (in mM): 77 $CsMeSO_4$, 38 CsCl, 1 EGTA, 5 HEPES, 1 3,4-DAP (pH 7.3), and the bath solution consisted of (in mM): 116 NaCl, 10 HEPES, 2 KCl, 1 $MgCl_2$, 10 $BaCl_2$, 1 3,4-DAP, 300 nM tetrodotoxin (pH 7.4). For all recordings, pipettes were pulled and filled as described above. Access resistance ranged from 8 to 12 MΩ and this was compensated for by 90%. Linear leak subtraction was performed using four waveforms of reverse polarity, each 25% of the size of the full waveform.

Drugs

The selective blockers of BK channels, iberiotoxin (IBTX; Sigma, St Louis, MO) and charybdotoxin (ChTX; Bachem, Torrence, CA), were used at 10–100 nM.[20,39] Stock solutions were made in 0.1 mg/ml cytochrome C dissolved in deionized H_2O and stored at −20°C. Both IBTX and ChTX were diluted into NFR before use. α-Bungarotoxin was obtained from Sigma, dissolved into bath saline, and used at 5 μg/ml. QX-314 was obtained from Alamone Laboratories (Jerusalem, Israel) and used at 5 mM; stock solutions of QX-314 (500 mM) were dissolved in deionized H_2O and aliquots were kept at −20°C until the day of use. All other reagents and chemicals were obtained from Sigma and dissolved into aqueous solutions.

Analysis

All acquisition and most analysis was done using the pClamp 6 suite of programs (Axon Instruments, Foster City, CA) running on a Pentium-based PC. Miniature endplate currents (mEPCs) were captured from recorded data using the Mini Analysis Program (Synaptosoft, Leonia, NJ). Additional analysis was done using Axograph 3.5 (Axon Instruments, Foster City, CA) on a Power Macintosh.

Experiments in which EPCs were measured were selected for analysis if the average of control EPCs was less than 5.2 nA. This was done to limit estimated peak voltage escape errors to less than 10%. The significance of the effects of BK blockers at each individual synapse studied was determined by comparing the amplitude of EPCs before and after BK channel blockade using Student's *t*-test. To test for significance in the mean effect at all synapses within a treatment group (IBTX, ChTX or vehicle control), we compared the distribution of the ratios (treated EPC/control EPC) to a theoretical population with a mean of one.

APs recorded from varicosities before and after perfusion with 100 nM IBTX were selected for analysis based on resting potential and the stability of the recordings. Experiments were eliminated from the data set if the peak of the AP showed significant rundown during perfusion with NFR. Sets of APs (three to 10) were averaged, and subsequent analysis was performed on these averaged APs. To reduce potential effects of differential sodium and potassium channel inactivation between individual APs recorded from each varicosity, sets of APs were chosen such that their resting potentials varied by no more than 1 mV and the average of the resting potentials fell between −60 and −65 mV. Significance of effects of IBTX on AP shape was determined using Student's *t*-test on the sets of APs that were selected for averaging. In all cases, $P < 0.05$ was considered statistically significant.

Numerical simulation

Nerve terminal APs were simulated according to Hodgkin and Huxley.[23] Voltage-dependent calcium currents (I_{Ca}) at the active zone were modeled by a third-order kinetic scheme:

$$I_{Ca} = \overline{g_{Ca}} p^3 (V_{az} - V_{Ca}),$$

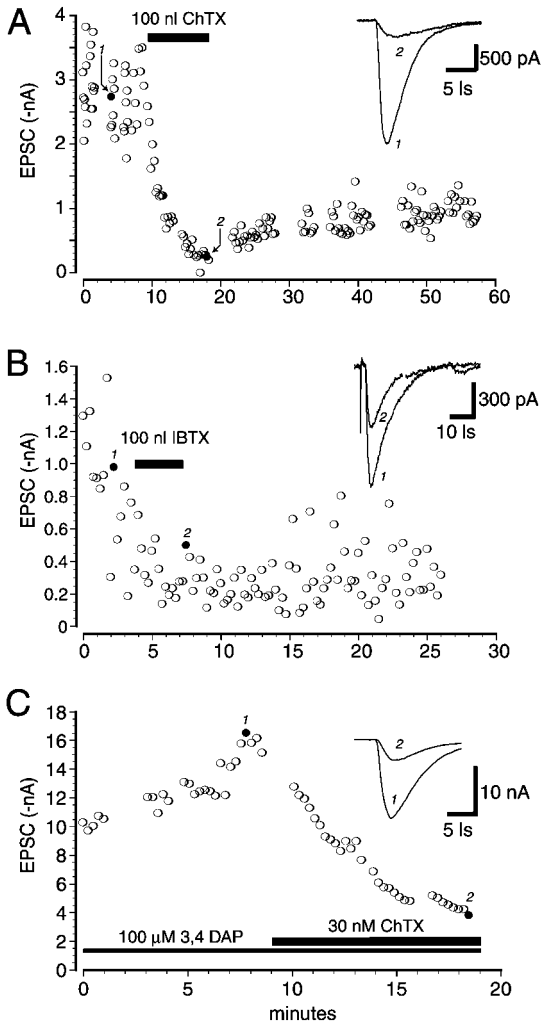

Fig. 1. Effects of potassium channel blockers on transmitter release. (A, B) Blockade of calcium-activated potassium current reduced transmitter release. Exposure of the nerve–muscle synapse to 100 nM ChTX (A) or 100 nM IBTX (B) reduced the amplitude of EPCs recorded from postsynaptic myocytes. Overall, application of ChTX decreased release by 32.7 ± 7.6% ($n = 15$) and application of IBTX decreased release by 39.7 ± 12% ($n = 7$). (C) Exposure to 3,4-DAP increased transmitter release, and this increase could be reversed by 30 nM ChTX. Insets: representative EPCs taken from the time points indicated in the plots by filled circles.

where $\overline{g_{Ca}}$ is the maximal conductance normalized for membrane area, p is a numerically integrated value according to the equation:

$$\frac{dp}{dt} = \alpha_p(1 - p) - \beta_p p$$

and V_{Ca} is the calcium reversal potential. The voltage dependencies of the "on" and "off" rate constants, respectively, are described by the following equations:

$$\alpha_p = 0.06(e^{((V_{az}+24)/14.5)})$$

$$\beta_p = 1.7/(e^{((V_{az}+34)/16.9)} + 1),$$

where V_{az} is the local active zone membrane potential. Values of the parameters in these equations were determined according to their ability to predict the kinetic features of I_{Ca} recorded at voltage-clamped *Xenopus* nerve terminals in response to step voltage changes.[68] I_{KCa} was calculated from the equation:

$$I_{KCa} = g_{KCa}(V_{az} - V_K),$$

where g_{KCa} was calculated according to the equations of Moczydlowski and Latorre[40] and the parameters of Hudspeth and Lewis,[25] and V_K is the potassium reversal potential. The Ca^{2+} concentration activating the g_{KCa} conductance[40] was calculated from I_{Ca} according to the equation $[Ca]_i = I_{Ca}/\pi FDd$,[47] where D, the diffusion coefficient, was set to 2×10^{-6} cm^2/s and the parameter d was set to the diameter of a membrane area representing summed active zone areas. The maximum values of g_{Ca} and g_{KCa} were set to preserve the ratio described by Hudspeth and Lewis,[25] while eliciting Ca^{2+} current magnitudes similar to the experimental data acquired in cultured *Xenopus* nerve terminals. The ratio of active zone membrane area (A_{az}) to the nerve terminal area (A_{nt}) and the series resistance (R_s) value were adjusted in order to simulate a significant electrical isolation of the Ca^{2+} and K_{Ca} channels in the active zone without influencing the overall membrane potential in the nerve terminal. Membrane capacitances were scaled according to area, assuming a specific value of 1 µF/cm^2. Numerical integrations were performed using SCoP (Simulated Research, Berrien Springs, MI).

RESULTS

Effect of BK channel blockade on evoked neurotransmitter release

Presynaptic nerve stimulation evoked EPCs of variable amplitude, which is characteristic of this preparation (see Fig. 1). Perfusion of the nerve–muscle synapse with ChTX (10–100 nM) decreased EPC amplitude by 32.7 ± 7.6% (mean ± S.E.M., $n = 15$; $P < 0.05$). Five of these 15 recordings showed no significant effect, while 10 had reductions that averaged 47%. Table 1 lists the effects of ChTX in individual recordings and Fig. 1A shows the time course of the effect of ChTX in a sample recording. In a separate set of experiments, bath perfusion with another selective BK antagonist, IBTX (100 nM), caused a significant decrease in EPC amplitude that averaged 39.7 ± 12% (mean ± S.E.M., $n = 7$; $P < 0.02$). Three of these seven recordings showed no significant effect, while four had reductions that averaged 64%. Table 1 outlines the specific effects of IBTX in individual recordings and Fig. 1B shows the time course of the effect of IBTX in a sample recording. To control for the potential effects of vehicle, the effects of lengthy bath perfusion with 0.1 mg/ml cytochrome c dissolved in NFR were examined and shown to have no significant effect on EPC amplitude ($n = 7$; see Table 1). In addition, perfusion with NFR had no effect on EPC amplitude ($n = 4$).

The effect of BK blockade on EPC amplitude contrasts with the effect of a blocker of voltage-gated potassium channels, 3,4-DAP (100 µM), which consistently increased the amplitude of EPCs recorded from postsynaptic muscle cells. A sample recording in which 3,4-DAP increased EPC amplitude is shown in Fig. 1C, and this increase was reversed by subsequent application of ChTX. Thus, despite the fact that blockers of voltage-gated potassium channels can increase EPC amplitude, selective blockers of BK channels can decrease EPC amplitude at this cultured nerve–muscle synapse.

We have performed several experiments that control for potential effects of IBTX and ChTX on our measure of transmitter release that go beyond their reported effect on BK channels. To test for possible postsynaptic effects at these embryonic synapses, we recorded mEPCs (in the

Table 1. Summary of the effects of various treatments on endplate current amplitude at individual synapses

Treatment	[Drug] (nM)	Control mean ± S.E.M. (−pA)	Drug-treated mean ± S.E.M. (−pA)	Change (%)
ChTX				
1	10	1809 ± 99	1113 ± 33	− 38.5*
2	10	1187 ± 63	672 ± 45	− 43.3*
3	10	3534 ± 95	2845 ± 100	− 19.5*
4	10	1688 ± 29	1630 ± 48	− 3.4
5	100	1161 ± 26	752 ± 49	− 35.2*
6	30	1601 ± 143	846 ± 134	− 47.1*
7	30	4256 ± 105	3977 ± 91	− 6.6
8	30	4666 ± 185	4439 ± 152	− 4.9
9	100	2481 ± 172	2425 ± 177	− 2.3
10	100	3902 ± 75	3417 ± 148	− 12.4*
11	30	5760 ± 239	708 ± 52	− 87.7*
12	30	1637 ± 195	1111 ± 119	− 32.2*
13	100	2722 ± 80	998 ± 57	− 63.3*
14	100	1269 ± 80	1217 ± 87	− 4.2
15	100	2847 ± 148	307 ± 27	− 89.2*
IBTX				
1	100	714 ± 126	296 ± 42	− 58.5*
2	100	4980 ± 160	5011 ± 294	+ 0.6
3	100	1015 ± 155	1027 ± 131	+ 1.1
4	100	1473 ± 219	1133 ± 291	− 23.1
5	100	3193 ± 153	1599 ± 128	− 49.9*
6	100	1522 ± 74	418 ± 59	− 72.5*
7	100	5176 ± 309	1251 ± 30	− 75.8*
Cytochrome C				
1	0.1 mg/ml	705 ± 44	621 ± 105	− 11.9
2	0.1 mg/ml	833 ± 95	805 ± 132	− 3.3
3	0.1 mg/ml	2474 ± 134	2582 ± 193	+ 4.4
4	0.1 mg/ml	4023 ± 329	3392 ± 424	− 15.7
5	0.1 mg/ml	2972 ± 380	2138 ± 303	− 28.1
6	0.1 mg/ml	2728 ± 742	2676 ± 597	− 1.9
7	0.1 mg/ml	3495 ± 272	3697 ± 266	+ 5.7
NFR				
1		1383 ± 196	1369 ± 142	− 1.0
2		2374 ± 226	2264 ± 122	− 4.6
3		3571 ± 236	3765 ± 295	+ 5.1
4		306 ± 22	301 ± 20	− 1.6

The mean EPC amplitude reported for each synapse was calculated by averaging the amplitudes of EPCs before and after each drug was applied. The asterisks indicate differences in the means that are statistically significant ($P < 0.05$).

presence of 1 μM tetrodotoxin) from postsynaptic muscle cells before and after exposure to 100 nM IBTX (Fig. 2A). The mean mEPC amplitude was not significantly affected by exposure to IBTX (253.5 ± 79.8 pA before and 270.5 ± 68.5 pA after exposure to IBTX, $n = 5$). A cumulative frequency plot of normalized mEPC amplitudes from five synapses before (open circles) and after (filled circles) IBTX application is shown in Fig. 2B. As a further test of possible postsynaptic effects of IBTX, a direct measurement was made of the effect of IBTX on acetylcholine (ACh)-activated receptor currents in myocytes. Fast perfusion[8] of ACh onto myocytes induced an inward current that was not affected by pretreatment with 100 nM IBTX. A representative example of ACh-activated current measured before and after exposure to 100 nM IBTX is shown in Fig. 2C. In four such experiments, there were no significant effects of IBTX on ACh-activated receptor currents (9.95 ± 1.75 nA control vs 9.88 ± 1.73 nA IBTX; mean ± S.E.M.).

In addition to examining the effect of the toxins on mEPC amplitude, we considered the possibility that BK channel blockade might alter directly the probability of transmitter release. To test this possibility, we examined the frequency of spontaneous mEPCs before and after application of 100 nM IBTX. The frequency of mEPCs before (open symbols) and after application of IBTX (filled symbols) in four separate nerve terminals (each represented by a different symbol shape) is plotted in Fig. 2D. The EPC amplitude in each of these four synapses was significantly reduced by IBTX. Although these synapses had different control mEPC frequencies, there was no significant effect of IBTX on the frequency of these events.

Finally, we considered the possibility that IBTX or ChTX could decrease EPC amplitude by partial blockade of presynaptic calcium channels. We tested the effect of IBTX or ChTX on calcium current evoked by depolarizing voltage steps. The two toxins had no significant effect on either somal or varicosity calcium current (Fig. 2E). We have found that the proportions of pharmacologically

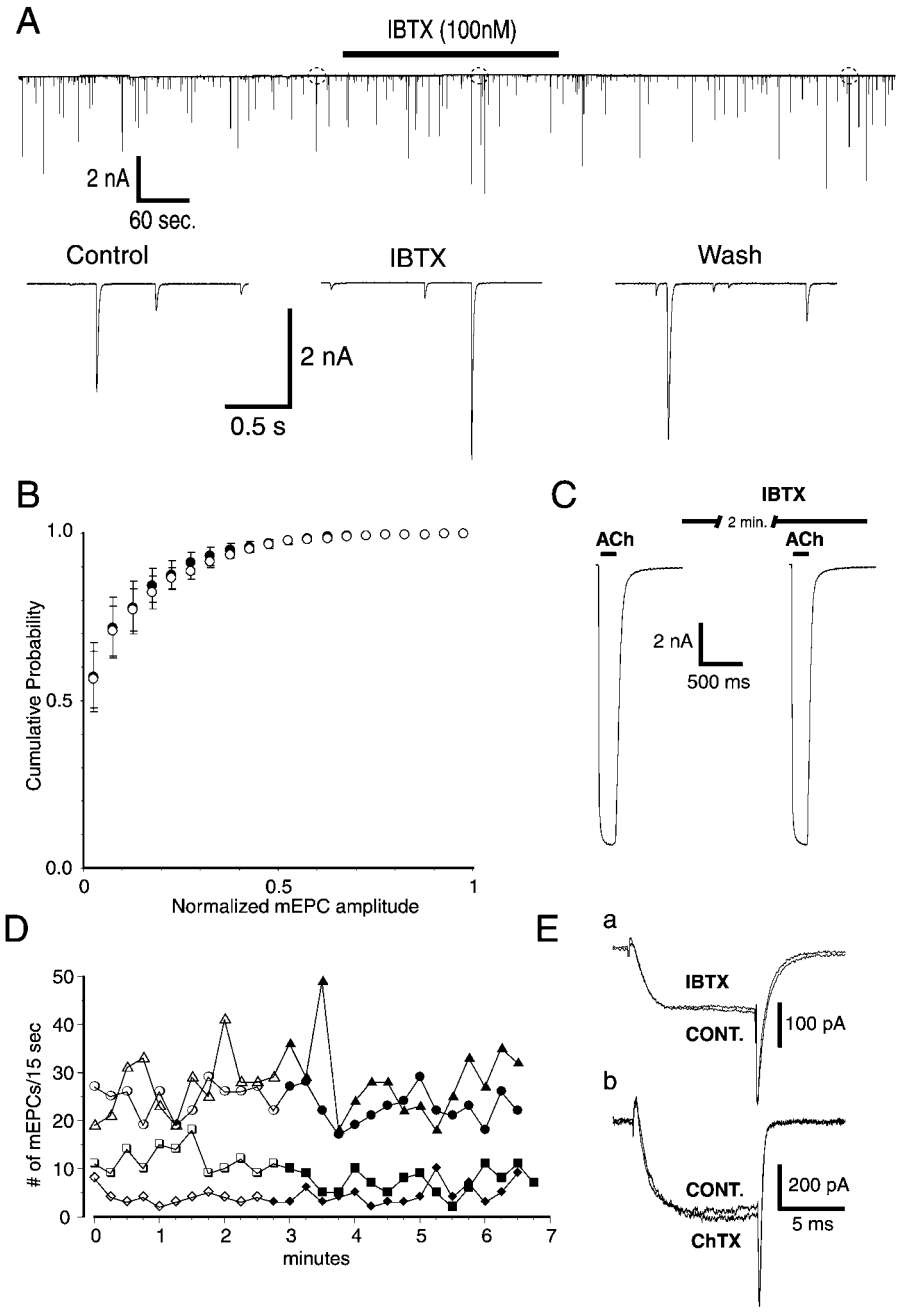

Fig. 2. Exposure to BK channel blockers does not affect ACh receptor current, calcium channel current or mEPC frequency. (A) mEPCs recorded from an innervated muscle (voltage clamped at −80 mV) in the presence and absence of IBTX. The lower graphs are 1-s sweeps of data taken from the areas indicated by the circles. (B) Normalized cumulative probability plot of mEPCs recorded from five nerve–muscle synapses before (open circles) and after (filled circles) a 10-min exposure to 100 nM IBTX. The amplitudes were normalized to the largest mEPC value in each recording. Symbols represent the mean ± S.E.M. (C) The inward current activated by application of ACh to a myocyte is not affected by perfusion with 100 nM IBTX. (D) The frequency of mEPCs is not affected by application of IBTX. Results from four different synapses (each represented by a different symbol shape) are shown. The *y*-axis indicates the number of mEPCs in 15-s bins recorded in the absence (open symbols) and presence (filled symbols) of 100 nM IBTX. EPC amplitude was significantly reduced in each of the four recordings shown. (E) Voltage-gated calcium current recorded from a neuron soma (step to +20 mV, $V_{hold} = -80$ mV) is not affected by 100 nM IBTX (a). Calcium channel current carried by barium recorded from a varicosity (step to +20 mV, $V_{hold} = -70$ mV) is not affected by 30 nM ChTX (b).

identified N-type calcium current in motoneuron somata and varicosities are similar (Poage and Meriney, unpublished observations). A representative example of calcium current evoked in a motoneuron soma before and after application of 100 nM IBTX is shown in Fig. 2Ea. In four such experiments, there were no significant effects on the magnitude of calcium current (338.2 ± 173.3 pA control vs 334.2 ± 169.6 pA IBTX). Similarly, Fig. 2Eb shows a representative example of calcium current evoked in a varicosity before and after

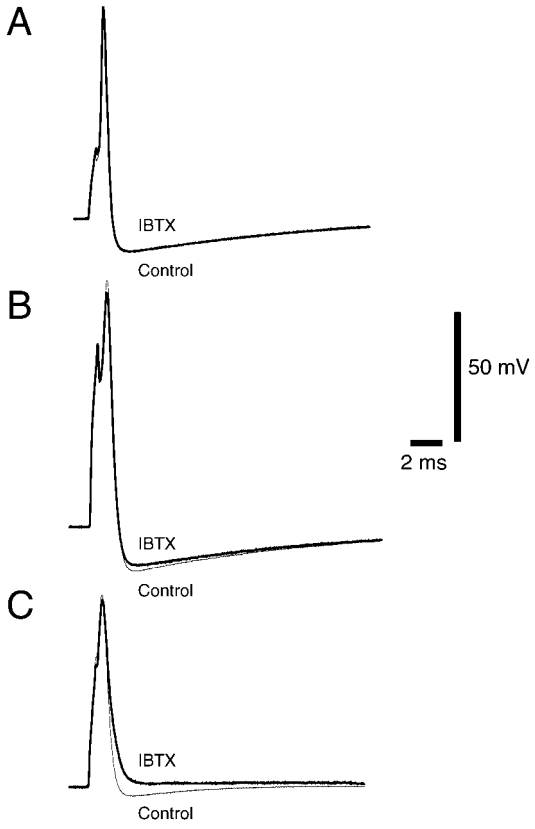

Fig. 3. Three representative effects of 100 nM IBTX on APs recorded from varicosities. IBTX had variable effects on AP waveforms that included no significant effect (A), a reduction in the amplitude of the afterhyperpolarization (B), and a broadening in the late phases of repolarization and a reduction in the afterhyperpolarization (C). Cumulative analysis from 12 such varicosities showed no significant effect of IBTX on AP shape.

application of 30 nM ChTX. In three such experiments, there were no significant effects on the magnitude of calcium current.

Effect of BK blockade on action potentials recorded at varicosities

Since we hypothesize that BK channels contribute significantly to the repolarization phase of the AP at the active zone, the effect of BK blockade on varicosity APs was examined. APs were recorded from 12 separate varicosities and the effects of 100 nM IBTX were examined following bath perfusion. IBTX had variable effects on AP shape recorded from varicosities. The range of the effects of IBTX on AP shape is shown in Fig. 3. In three recordings, no effect of IBTX was observed (Fig. 3A). In eight recordings, the peak of the AP varied slightly and/or the peak of the afterhyperpolarization decreased significantly (Fig. 3B). An unusual recording in which there was a significant broadening of the repolarizing phase of the AP and a large reduction in the amplitude of the afterhyperpolarization is shown in Fig. 3C. Although we observed the significant effects reported above in individual recordings, when the population of recordings was tested as a whole, there was no significant change in AP shape following IBTX exposure.

In summary, we observed significant reductions in EPC amplitude following BK channel blockade (Fig. 1, Table 1), but could not observe consistent significant effects on the AP waveform recorded from varicosities. Unlike voltage-clamp recordings of isolated calcium current, these recordings of AP shape were made in normal saline with all membrane conductances intact. Under these natural conditions, we hypothesize that the active zone patch of membrane that regulates transmitter release, and contains most of the calcium and BK channels in the varicosity, is isolated significantly from the site of AP recording. As such, it is difficult to observe effects of BK channel blockade on the whole varicosity AP.

Numerical simulations

As a test of the hypothesis that blockade of BK channels can modify the active zone AP shape and depress local Ca^{2+} entry without a consistent, measurable effect on the AP detected by our patch recordings, we developed a two-patch equivalent circuit model analogous to that of Taylor *et al.*[63] (also see Ref. 28). The equivalent circuit model illustrated in Fig. 4A contains two patches of membrane, each with its own conductance, separated by a series resistance ($R_s = 5\ \Omega\ cm^2$). One patch of membrane, representing the nerve terminal, contains Hodgkin and Huxley-type Na^+, K^+ and leak channels, and can produce an AP by simulated current injections. The second patch of membrane is smaller and represents the active zone membrane containing only Ca^{2+} and K_{Ca} channels; current flowing from the larger patch and from local active conductances is responsible for charging and discharging its membrane capacitance. The membrane potential across the large patch is denoted as the nerve terminal voltage (V_{nt}; Fig. 4A) and represents the voltage measured experimentally. V_{az} is the transmembrane voltage across the active zone membrane responsible for the activation of g_{Ca} and g_{KCa}. The model predictions of the two-patch model during an AP in the presence of K_{Ca} current (thick lines) and when g_{Kca} was reduced by 99% (thin lines) are illustrated in Fig. 4B. It can be observed that this reduction in the magnitude of g_{KCa} (see I_{KCa} trace in Fig. 4B) slightly decreases the rate of repolarization of the whole terminal AP (V_{nt}; Fig. 4B). However, the late repolarization phase of the local active zone voltage change (V_{az}; Fig. 4B) is significantly broadened. In both patches there is little or no change in the peak voltage. Moreover, the reduction in g_{KCa} reduces the rate of rise and peak of the calcium current (I_{Ca}; Fig. 4B).

The contrasting model predictions for the effects of a delayed rectifier blocker, such as 4-aminopyridine, which presumably acts upon delayed rectifier channels of the nerve terminal, are shown in Fig. 4C. It can be observed that a 10-fold reduction in g_K in the simulation leads to a significant prolongation of the AP in the whole nerve terminal and in the active zone (Fig. 4C, V_{nt} and V_{az}, respectively). This is in agreement with experimental

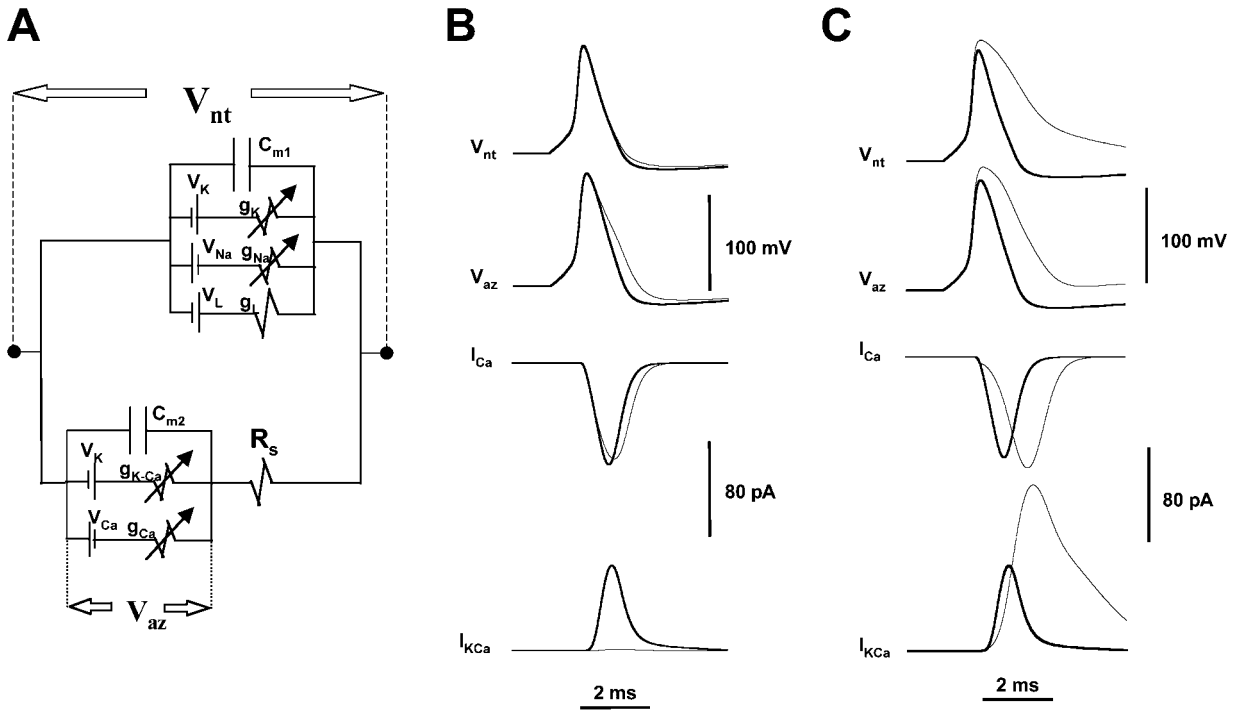

Fig. 4. Two-patch equivalent circuit model of the nerve terminal containing a partially isolated active zone membrane patch. (A) Equivalent circuit. The model includes voltage- and time-dependent conductances (g_{Na}, g_K) and a constant g_L, electrically isolated by a series resistance (R_s) from an active zone membrane patch with voltage- and time-dependent g_{Ca}, and a voltage-, time- and Ca^{2+}-dependent g_{KCa}. V_{nt} and V_{az} are the membrane potentials across the whole nerve terminal and the active zone patch, respectively; C_{m1} and C_{m2} are capacitances of the nerve terminal and active zone membrane patches, respectively; V_{Na}, V_K, V_L and V_{Ca} are reversal potentials for Na^+, K^+, leak and Ca^{2+} conductances, respectively. (B) Model simulation of the effects of BK channel blockade. Simulated time course of the variables V_{nt}, V_{az}, I_{Ca} and I_{KCa}, when the maximum g_{KCa} conductance is set to either 0.4 nS/μm^2 (thick trace) or 0.004 nS/μm^2 (thin trace). Nerve terminal membrane APs were elicited by 0.5-ms current steps of 100 pA. Other simulation parameters were set as follows: $V_{rest} = -60$ mV; $V_{Na} = 65$ mV; $V_K = -95$ mV; $V_L = -57$ mV; $V_{Ca} = 80$ mV; $g_{Na} = 0.6$ nS/μm^2; $g_K = 0.08$ nS/μm^2; $g_{Ca} = 0.1$ nS/μm^2; $g_L = 0.001$ nS/μm^2; $C_{m1} = 0.3$ pF; $C_{m2} = 0.015$ pF; $R_s = 5\ \Omega$ cm^2. (C) Model simulation of the effects of 4-aminopyridine. Simulated time course of the variables V_{nt}, V_{az}, I_{Ca} and I_{KCa}, when the maximum g_K conductance is set to either 0.08 nS/μm^2 (thick trace) or 0.008 nS/μm^2 (thin trace).

results.[50,67] Moreover, the prolongation of the AP is predicted to be associated with a marked increase in I_{Ca} (compare thick and thin I_{Ca} traces in Fig. 4C), which is also consistent with the potentiating effect of 4-aminopyridine on synaptic transmission. An interesting prediction of this simulation, which we have not yet confirmed, is the remarkable increase in I_{KCa} that should occur as a result of the g_K block and the concomitant AP prolongation.

Effect of action potential broadening on calcium influx at varicosities

Given the results of our numerical simulation, we sought to provide support for these hypotheses using direct recordings of varicosity calcium current activated by model AP waveforms under conditions that isolated calcium current by blocking sodium and potassium currents. The effects on varicosity calcium current when the sample APs displayed in Fig. 3C were used as voltage-clamp commands are illustrated in Fig. 5A. When these AP waveforms were used as voltage commands, the peak calcium current was slightly, but significantly, reduced by $4.0 \pm 0.9\%$, while the total calcium influx (integral) was significantly increased by $12.6 \pm 1.8\%$ (mean ± S.E.M., $n = 6$). Since this sample AP waveform may not faithfully represent the effects of IBTX on AP shape in the active zone region, we investigated the effects of systematic broadenings in the repolarization phase on a model AP waveform. This approach further elucidates the types of AP modification that would produce a decrease in peak calcium current and provides a basis for hypotheses related to the effects of BK channel blockade on EPC amplitude. As a template, a control varicosity AP was used as a model to construct simplified AP waveforms. The varicosity AP was scaled slightly such that it had a resting potential of −60 mV and a peak amplitude of +30 mV. The scaled AP was then modeled faithfully with a series of ramps up to the peak. The repolarizing phase was simplified to a single ramp to allow for consistent modification (Fig. 5B).[44] The repolarizing phase of the model waveform was broadened so that it reached the resting potential 1 ms later than the control waveform. This broadening was begun at 100-μs intervals in the repolarization. A sample recording of calcium currents activated using a control AP waveform and one that was broadened beginning at the peak are shown in Fig. 5C. Following AP broadening that began at the peak, calcium current amplitude was slightly increased by $3 \pm 1.8\%$ ($n = 6$).

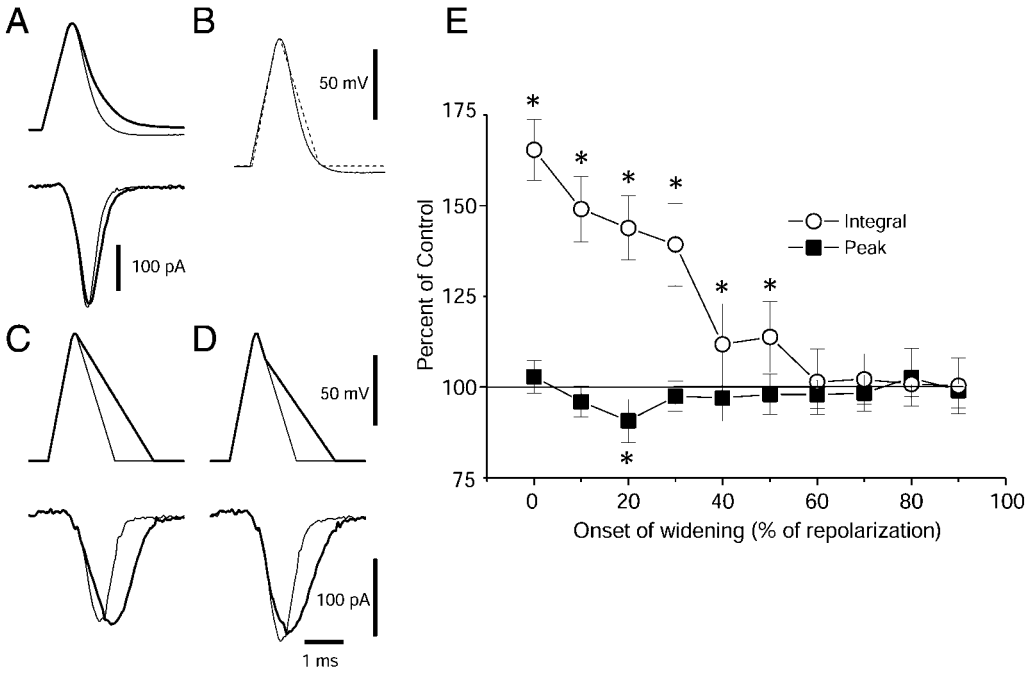

Fig. 5. Effects of AP broadening on barium current through calcium channels. (A) When the AP waveforms shown in Fig. 3C were used as voltage-clamp commands (top traces), peak barium current through calcium channels was slightly reduced, while total influx was increased (bottom traces). (B) A control AP waveform is shown (solid line) superimposed with the modeled waveform (dashed line) that was used for systematic broadening. (C) Representative example of the effect of broadening the model AP from the peak on barium current through calcium channels recorded from a varicosity. (D) Representative example of the effect of broadening the model AP starting at 20% of repolarization on barium current recorded from a varicosity. (E) Summary plot of the effects of AP broadening on peak barium current (squares) and total barium influx (integral; circles). The ratio of currents activated by broadened vs control APs was compared to a theoretical population (mean = 1) using the paired Student's *t*-test. $*P < 0.05$, significantly different ($n = 6$).

In contrast, Fig. 5D shows a sample recording of the effects on calcium current of using an AP waveform that was broadened beginning when repolarization was 20% complete. Following AP broadening that began during the repolarization phase of the AP, peak calcium current was decreased by $10 \pm 2.5\%$ ($n = 6$; Fig. 5D). The square symbols in Fig. 5E plot the effects on peak calcium current of AP waveforms in which broadening begins at various time points after the peak of the AP. Variations in the timing of the beginning of broadening revealed that when broadening was begun at 20% of AP repolarization, peak calcium current was maximally decreased (Fig. 5E, squares). In contrast, when total calcium influx was measured, broadening of the AP either had no effect (when broadening began later than 50% of AP repolarization) or increased total calcium influx (when broadening began before 50% of AP repolarization; Fig. 5E, circles). These effects are smaller than, but similar to those reported by Pattillo *et al.*[44] when AP waveforms of varying shape were broadened and used as voltage-clamp commands in chick ciliary ganglion cell somata.

DISCUSSION

We report a decrease in EPC amplitude following blockade of BK channels in *Xenopus* nerve–muscle co-cultures. This is in contrast to the effect of blockade of either BK channels[48] or voltage-gated potassium channels[41] on synaptic transmission at the adult frog neuromuscular junction. Indeed, in most preparations, blockade of potassium channels causes an increase in the duration of AP repolarization, increased calcium influx and increased transmitter release.[3,50,67] Similarly, in *Xenopus* varicosities, blockade of voltage-gated potassium channels by 3,4-DAP increased transmitter release magnitude (Fig. 1C).

Since IBTX or ChTX does not affect presynaptic calcium channels, postsynaptic ACh receptor sensitivity or spontaneous mEPC frequency, we postulate that these agents have specific effects on presynaptic BK channels at cultured *Xenopus* nerve–muscle synapses. We hypothesize that the decrease in EPC amplitude caused by BK channel blockade resulted from a broadening of the presynaptic AP that decreased the driving force for calcium entry, and that our inability to record a consistent effect on varicosity APs may be due to electrical isolation of the active zone membrane. Since BK channels have been shown to be co-localized with the calcium channels that regulate transmitter release,[68,69] we expect that BK channel expression may be restricted to highly localized active zone regions of the varicosity. The currents that flow in active zone regions of the varicosity may have a limited influence over the whole varicosity AP. In fact, optical detection of increases in intracellular calcium following AP invasion in these nerve terminals has revealed discrete microdomains of calcium influx.[16]

To evaluate this hypothesis, we developed a mathematical model using an equivalent circuit model of two patches of membrane: an active zone patch containing Ca^{2+} and K_{Ca} channels, and a nerve terminal (varicosity) patch containing Na^+, K^+ and leak channels (Fig. 4). The simulations predicted effects of BK channel blockade on calcium current and AP shape, and support our hypothesis that the active zone membrane patch may be partially isolated by a significant series resistance (R_s). This resistance could represent the electrical isolation imposed by a convergent current density in the cytoplasm between the recording site and the active zone. Recent observations using a combination of pre- and postsynaptic markers (DiGregorio *et al.*, unpublished observations) show that the separation between transmitter release specializations along *Xenopus* nerve–muscle contacts is ~10–20 μm, although it is possible that more than one active zone could exist within these areas of specialization. Thus, assuming cylindrical nerve terminals of ~2 μm in diameter and with an internal resistivity of 100 Ω cm,[24,47] the calculated access resistance to active zones could be approximately 1.6 MΩ. This is slightly smaller than the R_s value of 5 MΩ used in the model simulations. However, it is likely that narrowing of nerve terminal segments between the site of recording and the active zone, and/or a larger internal resistivity, could account for the difference. Other factors that may plausibly contribute to a relatively large R_s are the cloud of vesicles which surrounds the active zone[12,66] and the restricted space of the synaptic cleft, where the pre- and postsynaptic membranes are estimated to be 50–70 nm apart over areas of contact of about 6–12 μm^2.[12,66] This synaptic cleft is not unlike the Schwann cell "exit" clefts that are thought to give rise to a significant series resistance in the squid giant axon.[58] In fact, after adjusting for the difference in the resistivity of seawater[13] and NFR,[19] the predicted values of R_s are within the range that could predict our experimental observations.

From the above discussion, it is clear that the relative electrical isolation of the active zone membrane from the site of recording can be explained by the cable properties of the nerve terminal segments between the recording site and the active zone. In current-clamp conditions, the presence of unblocked membrane conductances would diminish measured changes in membrane voltage. Indeed, Poolos and Johnston[45] have recently shown a reduced effect of BK blockade on APs recorded in CA1 pyramidal cells with increasing distance from the cell soma (where the BK channels are likely to be clustered). We consider it likely that our current-clamp recordings of AP shape were at variable and unpredictable distances from the active zone. In contrast, under voltage-clamp conditions, the resistance of the membrane would be increased by pharmacological and ionic block of potassium and sodium conductances, thus increasing our ability to control the voltage at a more distant membrane. In this regard, our model is a two-membrane patch approximation of the more realistic distributed cable of the nerve terminal, including the varicosity and active zone.

Selective blockade of BK channels has previously been shown to broaden somal AP repolarization at relatively late phases in the AP as compared with voltage-gated potassium channel blockade. Depending on the cell type studied, selective BK channel blockade has been shown to cause AP broadening after the peak of the AP at various time points during the repolarizing phase.[14,52,55,59,70] To test the predictions of the numerical simulation and investigate the range of changes in AP shape that would result in decreased calcium current, several example AP waveforms were used as voltage-clamp commands in recordings of isolated calcium current from varicosities. When the repolarizing phase of an AP waveform was broadened beginning at different time points, it was found that the effect of broadening on the peak of the elicited calcium current was dependent on the precise timing of the initiation of broadening. Broadening that began at 20% of repolarization decreased peak calcium current by about 10%. AP broadening initiated after the peak of the AP is likely to have effects due primarily to decreased driving force and slowed calcium channel deactivation, rather than causing the activation of a greater number of channels.[44] Thus, we hypothesize that BK channel blockade reduces transmitter release at this synapse by decreasing the driving force for calcium during AP repolarization. Although our data indicate a relatively small decrease in peak calcium current using the model APs (about 10% when broadening from 20% of repolarization), transmitter release magnitude at the adult neuromuscular junction has been found to be proportional to calcium entry raised to the fourth power.[17] This would predict a roughly 35% decrease in transmitter release resulting from a 10% drop in calcium entry. The fact that we often observed a larger decrease in transmitter release may be due to a larger than fourth power relationship between calcium and transmitter release.[15,69] Recent experiments suggest that a fifth power relationship may exist at release sites in *Xenopus* varicosities,[69] which would predict a 40% decrease. Our numerical simulations and calcium current recordings suggest that the local effect of BK channels on AP shape at active zone regions of *Xenopus* nerve–muscle synapses can be explained by an acceleration of AP repolarization within a time window over which driving force effects on calcium influx predominate.[44] However, the precise effect of BK channel blockade on the natural AP shape at the active zone is likely to be similar, but not identical, to the waveforms we have tested here. Based on the magnitude of effects of BK channel blockade on release at many of the synapses studied, we hypothesize that peak calcium influx is altered to a greater extent than revealed using our model AP waveforms.

At the other end of the spectrum, the absence of effects of BK channel blockade in some recordings could be due to several issues. First, there may be developmental differences in the expression and coupling of BK channels at these embryonic synapses. In fact, Sugiura and Ko[60] have reported that BK channel blockade had no effect on adult 14-day regenerating frog neuromuscular junctions. Second, there may be heterogeneity among cultured cholinergic neurons that form synapses with

muscle in culture. Indeed, we have found that a significant fraction of neurons do not express measurable BK current (Yazejian and Grinnell, unpublished observations). We cannot distinguish *a priori* between different types of cholinergic neurons that might be present in this culture system, and as such, we cannot be sure that they are all expressing a similar complement of presynaptic ion channels. Third, recent studies have shown that expression of BK channel β-subunits can alter the sensitivity of these channels to scorpion toxins such that 10–30 nM ChTX may not provide complete blockade.[18] However, this seems unlikely in the case of BK channels in *Xenopus* varicosities, as their low calcium sensitivity suggests a lack of β-subunit expression.[37,69]

A further implication of the data presented here is that, during an AP at the embryonic *Xenopus* neuromuscular junction, the magnitude of transmitter release is regulated by the rate of calcium influx during the early part of the calcium current, and not the total AP-evoked calcium influx. The largest and most transient increases in intracellular Ca^{2+} concentration will occur near the mouth of the calcium channel,[2] and this local calcium transient will be the most sensitive to subtle changes in driving force. As such, the calcium sensors for transmitter release at this synapse may be relatively close to the calcium channels that open during an AP. Additional transmitter release triggered by the large amount of calcium that enters more slowly during the later phases of the AP-evoked calcium influx may be limited by the time required to dock or prime additional vesicles at release sites.

A decrease in transmitter release with AP broadening has also been observed at the neuromuscular junction of the jellyfish.[56] In that case, inactivation of A-type potassium channels led to AP broadening beginning just after the peak of the AP. This was followed by decreased excitatory junction potential amplitude. When these APs were used as voltage-clamp commands, the broadened APs elicited calcium current with decreased peak amplitude, increased time to peak and increased total calcium influx.[56] These observations are reminiscent of our data and provide an example of AP broadening decreasing peak calcium influx and transmitter release, while total calcium influx (integral) is increased.

Finally, it is interesting to note that we observed a decrease in transmitter release following BK channel blockade at embryonic *Xenopus* neuromuscular synapses, while Robitaille and Charlton[48] observed an increase in transmitter release at the adult frog neuromuscular junction. This difference could arise due to developmental changes in ion channel numbers or kinetics,[43,60] BK channel sensitivity to calcium[7] or AP shape. The data presented in Fig. 5 suggest that a shift in the timing of BK channel contribution from near the peak of the AP to 20% of repolarization could have opposite effects on peak calcium current and the magnitude of transmitter released. There may also be developmental changes in elements of presynaptic structure, such as the spatial relationship between calcium channels and calcium sensors. It will be interesting to examine possible developmental changes in the effects of BK blockade on transmitter release at these embryonic synapses in future studies.

Acknowledgements—We thank Robert Poage for many discussions and critical evaluation of the manuscript, and Jim Dilmore for his assistance with fast perfusion. This work was supported by NIH grants NS 32345 (S.D.M.), MH 18273 (J.M.P.), NS 30673 (A.D.G.) and AR 25201 (J.L.V.).

REFERENCES

1. Adams P. R., Constanti A., Brown D. A. and Clark R. B. (1982) Intracellular Ca^{2+} activates a fast voltage-sensitive K^+ current in vertebrate sympathetic neurones. *Nature* **296,** 746–749.
2. Adler E. M., Augustine G. J., Duffy S. N. and Charlton M. P. (1991) Alien intracellular calcium chelators attenuate neurotransmitter release at the squid giant synapse. *J. Neurosci.* **11,** 1496–1507.
3. Augustine G. J. (1990) Regulation of transmitter release at the squid giant synapse by presynaptic delayed rectifier potassium current. *J. Physiol.* **431,** 343–364.
4. Augustine G. J., Charlton M. P. and Smith S. J. (1985) Calcium entry and transmitter release at voltage-clamped nerve terminals of squid. *J. Physiol.* **367,** 163–181.
5. Augustine G. J., Charlton M. P. and Smith S. J. (1987) Calcium action in synaptic transmitter release. *A. Rev. Neurosci.* **10,** 633–693.
6. Bielefeldt K. and Jackson M. B. (1993) A calcium-activated potassium channel causes frequency-dependent action-potential failures in a mammalian nerve terminal. *J. Neurophysiol.* **70,** 284–298.
7. Blair L. A. and Dionne V. E. (1985) Developmental acquisition of Ca^{2+}-sensitivity by K^+ channels in spinal neurones. *Nature* **315,** 329–331.
8. Blanpied T. A., Boeckman F. A., Aizenman E. and Johnson J. W. (1997) Trapping channel block of NMDA-activated responses by amantadine and memantine. *J. Neurophysiol.* **77,** 309–323.
9. Borst J. G., Helmchen F. and Sakmann B. (1995) Pre- and postsynaptic whole-cell recordings in the medial nucleus of the trapezoid body of the rat. *J. Physiol.* **489,** 825–840.
10. Borst J. G. and Sakmann B. (1996) Calcium influx and transmitter release in a fast CNS synapse. *Nature* **383,** 431–434.
11. Borst J. G. G. and Sakmann B. (1998) Calcium current during a single action potential in a large presynaptic terminal of the rat brainstem. *J. Physiol.* **506,** 143–157.
12. Buchanan J., Sun Y. A. and Poo M. M. (1989) Studies of nerve–muscle interactions in *Xenopus* cell culture: fine structure of early functional contacts. *J. Neurosci.* **9,** 1540–1554.
13. Cole K. S. and Moore J. W. (1960) Liquid junction and membrane potentials of the squid giant axon. *J. gen. Physiol.* **43,** 971–980.
14. Davies P. J., Ireland D. R. and McLachlan E. M. (1996) Sources of Ca^{2+} for different Ca^{2+}-activated K^+ conductances in neurones of the rat superior cervical ganglion. *J. Physiol.* **495,** 353–366.
15. Delaney K, Tank D. W. and Zucker R. S. (1991) Presynaptic calcium- and serotonin-mediated enhancement of transmitter release at crayfish neuromuscular junction. *J. Neurosci.* **11,** 2631–2643.
16. DiGregorio D. A. and Vergara J. L. (1997) Localized detection of action potential-induced presynaptic calcium transients at a *Xenopus* neuromuscular junction. *J. Physiol.* **505,** 585–592.

17. Dodge F. A. Jr. and Rahamimoff R. (1967) Co-operative action of calcium ions in transmitter release at the neuromuscular junction. *J. Physiol.* **193,** 419–432.
18. Dworetzky S. I., Boissard C. G., Lum-Ragan J. T., McKay M. C., Post-Munson D. J., Trojnacki J. T., Chang C.-P. and Gribkoff V. K. (1996) Phenotypic alteration of a human BK (*hSlo*) channel by *hSlo*β subunit coexpression: changes in blocker sensitivity, activation/relaxation and inactivation kinetics, and protein kinase A modulation. *J. Neurosci.* **16,** 4543–4550.
19. Falk G. and Fatt P. (1964) Linear electrical properties of striated muscle fibers observed with intracellular electrodes. *Proc. R. Soc. Lond., Ser. B* **160,** 69–123.
20. Galvez A., Gimenez-Gallego G., Reuben J. P., Roy-Contancin L., Feigenbaum P., Kaczorowski G. J. and Garcia M. L. (1990) Purification and characterization of a unique, potent, peptidyl probe for the high conductance calcium-activated potassium channel from venom of the scorpion *Buthus tamulus*. *J. biol. Chem.* **265,** 11,083–11,090.
21. Gingrich K. J., Beardsley D. and Yue D. T. (1993) Ultra-deep blockade of Na^+ channels by a quaternary ammonium ion: catalysis by a transition-intermediate state? *J. Physiol.* **471,** 319–341.
22. Heidelberger R., Heinemann C., Neher E. and Matthews G. (1994) Calcium dependence of the rate of exocytosis in a synaptic terminal. *Nature* **371,** 513–515.
23. Hodgkin A. L. and Huxley A. F. (1952) A quantitative description of membrane current and its application to conduction and excitation in nerve. *J. Physiol.* **117,** 500–544.
24. Hodgkin A. L. and Nakajima S. (1972) Analysis of the membrane capacity in frog muscle. *J. Physiol.* **221,** 121–136.
25. Hudspeth A. J. and Lewis R. S. (1988) Kinetic analysis of voltage- and ion-dependent conductances in saccular hair cells of the bull-frog, *Rana catesbeiana*. *J. Physiol.* **400,** 237–274.
26. Hulsizer S. C., Meriney S. D. and Grinnell A. D. (1991) Calcium currents in presynaptic varicosities of embryonic motoneurons. *Ann. N. Y. Acad. Sci.* **635,** 424–428.
27. Katz B. (1969) *The Release of Neural Transmitter Substances*. Liverpool University Press, Liverpool.
28. Keynes R. D., Rojas E., Taylor R. E. and Vergara J. (1972) Calcium and potassium systems of a giant barnacle muscle fiber under membrane potential control. *J. Physiol.* **229,** 409–455.
29. Kidokoro Y. and Sand O. (1989) Action potentials and sodium inward currents of developing neurons in *Xenopus* nerve–muscle cultures. *Neurosci. Res.* **6,** 191–208.
30. Lancaster B., Nicoll R. A. and Perkel D. J. (1991) Calcium activates two types of potassium channels in rat hippocampal neurons in culture. *J. Neurosci.* **11,** 23–30.
31. Lim N. F., Nowycky M. C. and Bookman R. J. (1990) Direct measurement of exocytosis and calcium currents in single vertebrate nerve terminals. *Nature* **344,** 449–451.
32. Lindgren C. A. and Moore J. W. (1989) Identification of ionic currents at presynaptic nerve endings of the lizard. *J. Physiol.* **414,** 201–222.
33. Lindgren C. A. and Moore J. W. (1991) Calcium current in motor nerve endings of the lizard. *Ann. N. Y. Acad. Sci.* **635,** 58–69.
34. Llinas R., Steinberg I. Z. and Walton K. (1981) Relationship between presynaptic calcium current and postsynaptic potential in squid giant synapse. *Biophys. J.* **33,** 323–351.
35. Magistretti J., Mantegazza M., Guatteo E. and Wanke E. (1996) Action potentials recorded with patch-clamp amplifiers—are they genuine? *Trends Neurosci.* **19,** 530–534.
36. McManus O. B. (1991) Calcium-activated potassium channels: regulation by calcium. *J. Biomembr. Bioenerg.* **23,** 537–560.
37. McManus O. B., Helms L. M. H., Pallanck L., Ganetzky B., Swanson R. and Leonard R. J. (1995) Functional role of the β subunit of high conductance calcium-activated potassium channels. *Neuron* **14,** 645–650.
38. Meriney S. D., Hulsizer S. C. and Grinnell A. D. (1991) Calcium currents in varicosities of motoneuron neurites ending on muscle cells *in vitro*. *Biomed. Res.* **12,** 53–55.
39. Miller C., Moczydlowski E., Latorre R. and Phillips M. (1985) Charybdotoxin, a protein inhibitor of single Ca^{2+}-activated K^+ channels from mammalian skeletal muscle. *Nature* **313,** 316–318.
40. Moczydlowski E. and Latorre R. (1983) Gating kinetics of Ca^{2+}-activated K^+ channels from rat muscle incorporated into planar lipid bilayers. Evidence for two voltage dependent Ca^{2+} binding reactions. *J. gen. Physiol.* **82,** 511–542.
41. Molgo J., Lemeignan M. and Lechat P. (1977) Effects of 4-aminopyridine at the frog neuromuscular junction. *J. Pharmac. exp. Ther.* **203,** 653–663.
42. Niewkoop P. D. and Faber J. (1967) *Normal Table of* Xenopus laevis *(Daudin)*. North-Holland, Amsterdam.
43. O'Dowd D. K., Ribera A. B. and Spitzer N. C. (1988) Development of voltage-dependent calcium, sodium, and potassium currents in *Xenopus* spinal neurons. *J. Neurosci.* **8,** 792–805.
44. Pattillo J. M., Artim D. E., Simples J. E. Jr and Meriney S. D. (1999) Variations in onset of action potential broadening: effects on calcium current studied in chick ciliary ganglion neurons. *J. Physiol.* **514,** 719–728.
45. Poolos N. P. and Johnston D. (1999) Calcium-activated potassium conductances contribute to action potential repolarization at the soma but not the dendrites of hippocampal CA1 pyramidal neurons. *J. Neurosci.* **19,** 5205–5212.
46. Rae J., Cooper K., Gates P. and Watsky M. (1991) Low access resistance perforated patch recordings using amphotericin B. *J. Neurosci. Meth.* **37,** 15–26.
47. Roberts W. M., Jacobs R. A. and Hudspeth A. J. (1990) Colocalization of ion channels involved in frequency selectivity and synaptic transmission at presynaptic active zones of hair cells. *J. Neurosci.* **10,** 3664–3684.
48. Robitaille R. and Charlton M. P. (1992) Presynaptic calcium signals and transmitter release are modulated by calcium-activated potassium channels. *J. Neurosci.* **12,** 297–305.
49. Robitaille R., Garcia M. L., Kaczorowski G. J. and Charlton M. P. (1993) Functional colocalization of calcium and calcium-gated potassium channels in control of transmitter release. *Neuron* **11,** 645–655.
50. Sabatini B. L. and Regehr W. G. (1997) Control of neurotransmitter release by presynaptic waveform at the granule cell to Purkinje cell synapse. *J. Neurosci.* **17,** 3425–3435.
51. Sah P. (1996) Ca^{2+}-activated K^+ currents in neurones: types, physiological roles and modulation. *Trends Neurosci.* **19,** 150–154.
52. Sah P. and McLachlan E. M. (1992) Potassium currents contributing to action potential repolarization and the afterhyperpolarization in rat vagal motoneurons. *J. Neurophysiol.* **68,** 1834–1841.
53. Sivaramakrishnan S., Bittner G. D. and Brodwick M. S. (1991) Calcium-activated potassium conductance in presynaptic terminals at the crayfish neuromuscular junction. *J. gen. Physiol.* **98,** 1161–1179.
54. Sivaramakrishnan S. and Laurent G. (1995) Pharmacological characterization of presynaptic calcium currents underlying glutamatergic transmission in the avian auditory brainstem. *J. Neurosci.* **15,** 6576–6585.
55. Solaro C. R., Prakriya M., Ding J. P. and Lingle C. J. (1995) Inactivating and noninactivating Ca^{2+}- and voltage-dependent K^+ current in rat adrenal chromaffin cells. *J. Neurosci.* **15,** 6110–6123.

56. Spencer A. N., Przysiezniak J., Acosta-Urquidi J. and Basarsky T. A. (1989) Presynaptic spike broadening reduces junctional potential amplitude. *Nature* **340,** 636–638.
57. Stanley E. F. and Goping G. (1991) Characterization of a calcium current in a vertebrate cholinergic presynaptic nerve terminal. *J. Neurosci.* **11,** 985–993.
58. Stimers J. R., Bezanilla F. and Taylor R. E. (1987) Sodium channel gating currents. Origin of the rising phase. *J. gen. Physiol.* **89,** 521–540.
59. Storm J. F. (1987) Action potential repolarization and a fast after-hyperpolarization in rat hippocampal pyramidal cells. *J. Physiol.* **385,** 733–759.
60. Sugiura Y. and Ko C.-P. (1997) Novel modulatory effect of L-type calcium channels at newly formed neuromuscular junctions. *J. Neurosci.* **17,** 1101–1111.
61. Tabti N. and Poo M.-M. (1991) Culturing spinal neurons and muscle cells from *Xenopus* embryos. In *Culturing Nerve Cells* (eds Banker G. and Goslin K.). MIT, Cambridge, MA.
62. Takahashi T., Forsythe I. D., Tsujimoto T., Barnes-Davies M. and Onodera K. (1996) Presynaptic calcium current modulation by a metabotropic glutamate receptor. *Science* **274,** 594–597.
63. Taylor R. E., Moore J. W. and Cole K. S. (1960) Analysis of certain errors in squid axon voltage clamp measurements. *Biophys. J.* **1,** 161–202.
64. Toth P. T. and Miller R. J. (1995) Calcium and sodium currents evoked by action potential waveforms in rat sympathetic neurones. *J. Physiol.* **485,** 43–57.
65. Wang G., Thorn P. and Lemos J. R. (1992) A novel large-conductance Ca(2 +)-activated potassium channel and current in nerve terminals of the rat neurohypophysis. *J. Physiol.* **457,** 47–74.
66. Weldon P. R. and Cohen M. W. (1979) Development of synaptic ultrastructure at neuromuscular contacts in an amphibian cell culture system. *J. Neurocytol.* **8,** 239–259.
67. Wheeler D. B., Randall A. and Tsien R. W. (1996) Changes in action potential duration alter reliance of excitatory synaptic transmission on multiple types of Ca^{2+} channels in rat hippocampus. *J. Neurosci.* **16,** 2226–2237.
68. Yazejian B., DiGregorio D. A., Vergara J. L., Poage R. E., Meriney S. D. and Grinnell A. D. (1997) Direct measurements of presynaptic calcium and calcium-activated potassium currents regulating neurotransmitter release at cultured *Xenopus* nerve–muscle synapses. *J. Neurosci.* **17,** 2990–3001.
69. Yazejian B., Sun X. P. and Grinnell A. D. (2000) Tracking presynaptic Ca^{2+} dynamics during neurotransmitter release with Ca^{2+}-activated K^+ channels. *Nature Neurosci.* **3,** 566–571.
70. Zhang L. and McBain C. J. (1995) Potassium conductances underlying repolarization and after-hyperpolarization in rat CA1 hippocampal interneurones. *J. Physiol.* **488,** 661–672.

(*Accepted* 4 *October* 2000)